RSC Advances

ROYAL SOCIETY OF CHEMISTRY

www.rsc.org/advances

Non-enzymatic detection of bilirubin based on Graphene – polystyrene sulfonate composite

T Balamurugan, Sheela Berchmans

Reduced Graphene oxide – poly styrene sulfonate (RGO-PSS) modified GC electrode for the detection of bilirubin.

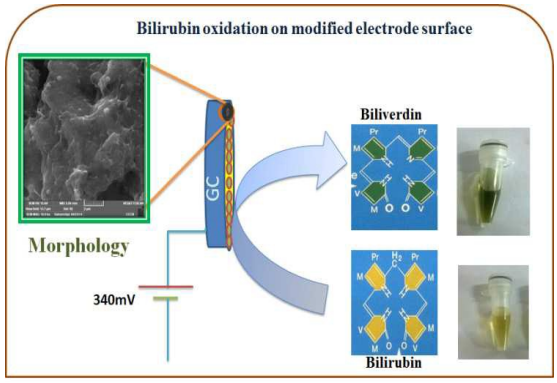

Journal Name

ARTICLE

Non-enzymatic detection of bilirubin based on Graphene – polystyrene sulfonate composite

Received 00th January 20xx,
Accepted 00th January 20xx

DOI: 10.1039/x0xx00000x

www.rsc.org/

T Balamurugan,[a] Sheela Berchmans,[a]*

We report, a selective, non-enzymatic bilirubin (BR) detection through catalytic oxidation on reduced graphene oxide (RGO) – Poly styrene sulfonate (PSS) composite film spin coated on Glassy carbon electrode. The catalytic ability, stability, morphology and composition of RGO-PSS composite, were evaluated using voltammetric, spectroscopic and microscopic techniques. The experimental variables influencing the analysis of bilirubin were optimized in terms of active material composition, pH and serum albumin concentration in blood. At the optimized condition, the linear dynamic range was found to be 0 - 450 µM, with a sensitivity of 0.16 µA μM^{-1} cm^{-2} and the detection limit was 2.0 µM. The modified electrode possesses good stability, reproducibility and selectivity towards bilirubin determination. The real sample analysis demonstrates the scope of the RGO-PSS composite modified electrode for practical clinical diagnosis.

Introduction

Bilirubin (BR) is a pathogenic yellow color pigment with tetra pyrrole units and is the by-product of normal breakdown of old red blood cells[1]. BR has both natural antioxidant and toxic properties under certain conditions[2]. BR circulates in the blood in two forms viz., conjugated (often referred to as direct) and unconjugated. Conjugated BR forms complex with glucoronic acid to form water soluble BR while unconjugated BR binds to albumin forming water soluble BR. A tiny fraction of free BR (non-albumin bound) also exists which is an important indicator for bilirubin toxicity. The free bilirubin is toxic to plasma[3].High concentrations of free bilirubin can evoke hepatic or biliary tract dysfunction and permanent brain damage or death in more-severe cases[4]. This free unconjugated BR exhibits a wide range of toxicity particularly towards neuronal cells which is neutralized by its ability to bind with albumin[5]. If untreated, the elevated level of BR causes jaundice associated with liver diseases such as cirrhosis, hepatitis, and hemolysis. High concentrations of unconjugated free BR in neonates can lead to Kernicterus (brain damage and hearing loss) and even death[6]. Low level of BR concentration is associated with anaemia and coronary artery diseases[3]. Neonatal jaundice is extremely common as almost every newborn infant child develops an unconjugated BR level greater than 340 µM/L during the first week of life, generally considered as dangerous[7]. Therefore, considering the diagnostic significance of BR, the accurate measurement of free bilirubin is clinically important and the development of an inexpensive analytical device for its detection is of great interest. The normal level of direct bilirubin is 0 - 0.3 mg/dl and total bilirubin is 0.3 (5.1 µM) to 1.9 mg/dl (34.2 µM) [6].

Various methods have been developed to detect BR. The most common spectroscopic measurement of bilirubin suffers due to interference from other proteins[8]. Diazo reaction based bilirubin sensor is compromised because of its pH dependence [9]. Polarography,[10] fluorometry and colorimetry[11] can also be used to detect this metabolite. The enzyme, bilirubin oxidase (BOD) catalyzes bilirubin to biliverdin (BV) in the presence of molecular oxygen. Amperometric biosensor based on BOD has been reported for bilirubin detection by measurement of decreasing levels of molecular oxygen[12] or oxidation of H_2O_2 [13]. These biosensors suffer from decreasing O_2 content than other active species and oxidation of H_2O_2 is not formed stoichiometrically with respect to BR but it depends on molecular O_2 content in the system[14]. Further BOD is expensive and unstable (50% activity lost in 17 h at 37°C). The immobilization of BOD requires stable matrix to maintain the required activity of tri nuclear copper redox Centre (TNC) [1]. Thus it is necessary to develop a stable biosensor for total bilirubin. The use of conducting polymer,[3] graphene, CNT and their composite with metal nanoparticles is being resorted to develop mediatorless and enzymeless sensing protocols. Graphene has attracted tremendous attention in sensor applications because of its fascinating properties such as large surface area, excellent chemical/thermal stability and superior electrical conductivity[15]. Because of its superior properties, graphene can be used for the functionalization of electrode surface to improve catalytic activity[16]. Further, the Graphene lattice is composed of two equivalent sub-lattice of carbon atoms bonded together with σ bonds and has π orbital that contribute delocalization of electrons within networks[17]. Poly

[a] CSIR-Central Electrochemical Research Institute, Karaikudi-630006, Tamilnadu, India

* Corresponding author E mail sheelaberchmans@yahoo.com or sheelab@cecri.res.in

styrene sulphonic acid and carbon nano material such as CNT and graphene were proved to be potential candidates in many biological applications like cholesterol detection[18], dopamine detection[19] and reduction of H_2O_2[20].

In this work, we report a selective non-enzymatic, electrochemical bilirubin sensor using reduced graphene oxide (RGO)–Poly styrene sulfonic acid (PSS) composite; spin coated on glassy carbon electrode (GC) in order to measure normal and hyperbilirubinemia levels of free bilirubin. The RGO-PSS composite prepared by us, can be easily dispersed in aqueous solution and is found to be quite stable for more than six months. The RGO-PSS modified electrode exhibited very good electrocatalytic properties besides its good conductivity and excellent stability upon cycling and was found to be a good sensing material for the detection of free bilirubin without interferences (scheme 1) The proposed method can be tuned to measure bilirubin in normal levels and hyperbilirubinemia by running the calibration experiment in the absence and presence of human serum albumin.

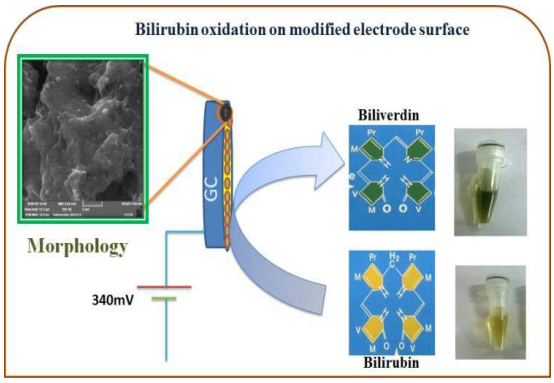

Scheme1: Schematic diagram of the reduced Graphene oxide – poly styrene sulfonate (RGO-PSS) modified GC electrode used for the detection of bilirubin.

Experimental Procedure

Materials

Graphite powder (< 20 µm), hydrazine monohydrate, human serum albumin (lyophilized powder, 97%) and ascorbic acid (≥ 99.5%) were purchased from Sigma Aldrich. H_2O_2 (30%) was procured from Nice chemicals, India. $NaNO_3$, glucose (≥ 99%), cholesterol (98%) and bilirubin (99%) were purchased from Hi media. Tris (hydroxymethyl) amino methane (Sisco Research Laboratories, India), Sodium salt of Poly (styrene sulfonic acid), M.W.70000 from Alfa aesar and glassy carbon (GC) disk electrode (3 mm dia.) and Platinum foil from CH Instruments inc. were used. The other reagents used in this work were analytical reagents. Ultrapure milli-Q water (having a resistivity of 18.2 MΩ cm^{-1}) was used throughout this study.

Methods

All electrochemical studies were carried out using Metrohm Autolab (PGSTAT302N, 30V/2000mA) potentiostat/Galvanostat with GPES 4.9002 version in a standard three electrode electrochemical cell with GC (ϕ = 3mm), platinum foil and NCE (Hg/Hg_2Cl_2, 1M KCl) as working, counter and reference electrodes respectively. The electrochemistry of bilirubin (BR) was investigated by cyclic voltammetry (CV) and amperometry. All the experiments were carried out under aerobic conditions at room temperature. The SEM and EDAX for the modified electrodes were obtained with the equipments from TESCAN, USA and TEM (TECNAI-G2 220 FEI model, operating voltage 200 KeV, USA). FTIR spectra were obtained using a Bruker Tensor 27 spectrophotometer. The UV-Visible spectra were obtained using a Perkin Elmer spectrophotometer (scan lambda 650, USA) and laser Raman spectrum was recorded using Renishaw Raman system 2000 model that employs 514 nm argon laser source. To confirm the performance of the sensor, bilirubin concentration in the serum sample was compared with the results from a commercial bilirubin-monitoring analyzer which adopts Jendrassik-Grof method.

Preparation of Graphene oxide (GO) using modified Hummer's method

Graphene oxide (GO) was prepared using previously reported modified Hummer's method.[22] RGO-PSS composite material was prepared based on a previous reported procedure with a slight modification [23]. Typically GO (0.1% in water, 250 mL) was dispersed homogeneously by sonication. N, N-dimethylformamide (50 mL) was added for further homogenization. To this resulting solution Hydrazine monohydrate (98 %, 50 µL) was added and stirred for 4 h at 80 – 90 ºC causing reduction of GO to reduced graphene oxide (RGO). Then stirring was continued overnight with 30 mL of 1% sodium salt of Poly (styrene sulfonic acid), PSS to produce black dispersion of RGO-PSS composite and filtered through 0.2 µm membrane filter, washed several times with water, and dried at room temperature. The RGO-PSS (0.1 %) composite was re-dispersed in water.

Modification of the glassy carbon electrode by RGO-PSS

The surface of Glassy carbon (GC) working electrode was fine polished over alumina slurry (0.05 µm mesh) followed by washing with milli-Q water and sonication in ethanol to remove any adsorbed species. At the end, the electrode was washed with water to remove ethanol. An optimized volume of 0.1% RGO-PSS (7 µL) composite was spin coated at 1000 rpm on the surface of GC and dried in vacuum desiccator for 48 h. Then the modified electrode was then washed with water to remove unbound material and henceforth designated as GC/RGO-PSS and stored at room temperature under inert atmosphere when not in use.

Results and Discussions

Characterization of RGO and RGO-PSS Composite

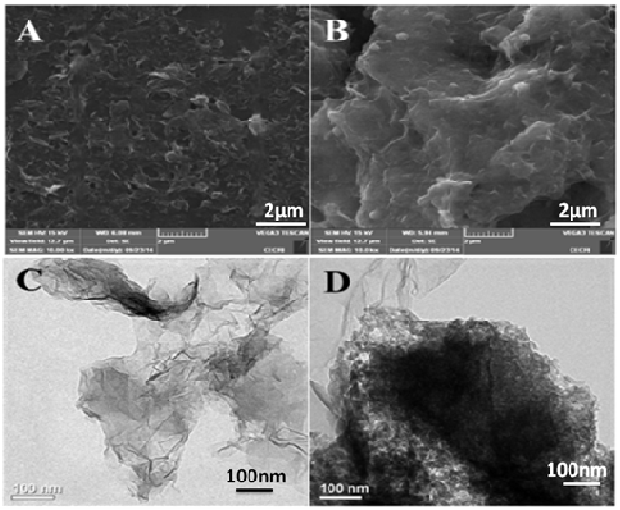

Fig.1. SEM images of (A) GC-RGO, (B) GC-RGO-PSS and TEM images of (C) GC-RGO, and (D) GC-RGO-PSS

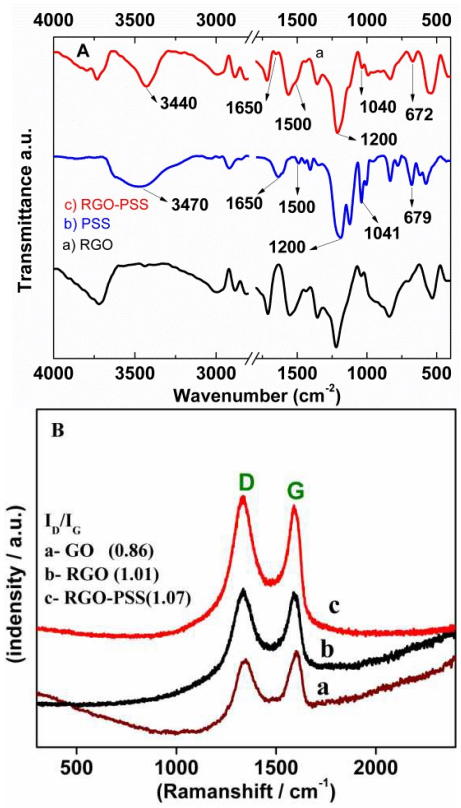

Fig.2.FTIR spectrum of 2A a) RGO; b) PSS; c) RGO-PSS. (B) Raman spectra of a) GO, (b) RGO, and (c) RGO-PSS composite.

The morphological features observed using SEM and TEM are presented in Fig.1. Fig.1A corresponds to the SEM image of GC/RGO and 1B corresponds to that of GC surface modified by RGO - PSS respectively. The SEM images clearly show morphology variation between Fig. 1A & B confirming the presence of PSS in the composite modified electrode. Bare GC electrode exhibits smooth uniform surface (SI Fig. S1A) while GC/RGO shows inter connected RGO sheets coated uniformly on the GC electrode and Fig. 1B shows the cloud like morphology of RGO-PSS composite confirming that PSS has been grafted on the RGO sheets. The TEM micrograph also confirms that the RGO sheets are homogeneously dispersed in solution and are quite smooth as shown in Fig. 1C. The PSS has been uniformly distributed on the RGO thin sheets as revealed by Fig.1D. EDAX analysis indicates that the composite contains carbon, oxygen and sulphur (SI Fig. S1B). This confirms that the poly (styrene sulfonate) is grafted on the RGO film.

In order to determine if the PSS has been grafted onto the RGO, FTIR spectra of RGO, PSS and RGO-PSS were taken and the results are presented in Fig. 2A. In the case of PSS, the IR spectrum shows a peak at 3470 cm^{-1} and 1650 cm^{-1} corresponding to O-H stretching vibration and bending vibration of water molecule [24]. The peak observed at 1042 cm^{-1} and 1200 cm^{-1} corresponds to O=S=O and SO_3^- symmetric stretching vibration respectively . The peaks at 1500 cm^{-1} are attributed to characteristic absorption peaks for benzene and the two peaks in the fingerprint region indicate para-substitution of sodium sulfonate. The peaks between 1000 and 1250 cm^{-1} are characteristic of C-C absorption for a carbon skeleton in a macromolecular chain. The peaks observed at 679, 1500 and 1650 cm^{-1} overlap with those of PSS. The IR spectrum of the RGO-PSS exhibits the same characteristic absorption peaks as PSS. These results indicate that PSS has been grafted onto the surface of graphene.

Raman spectroscopy is often used to evaluate the quality of carbon materials. Fig. 2B shows the Raman spectra of GO, RGO and RGO-PSS. The Raman spectra of GO has wide peaks around 1600 (G) and 1340 cm^{-1} (D). The increase in D band intensity indicates the reduction in size of the in-plane sp^2 domains, possibly due to the extensive oxidation. The Raman spectrum of the RGO also contains both G and D bands (at 1590 and 1330 cm^{-1}, respectively) with an increased D/G intensity ratio (1.01) compared to that in GO. This change suggests a decrease in the sp^2 carbon domains upon reduction of the exfoliated GO. RGO-PSS also has these D and G peaks but the D/G intensity ratio (1.07) is greater than that in the GO (0.86) spectrum indicating higher disorder due to PSS grafting.

UV-Vis spectrum of composite material also reveals the typical features expected of GO and RGO (SI Fig.S1C). GO exhibits absorption peak at 230 nm and 300 nm due to π-π* and n- π* transitions respectively and the absorption peak of the π-π* shifts to 270 nm for RGO [25] indicating the removal of oxygen functional group and increasing conjugation structure in support of the reduction of GO. The RGO-PSS composite shows the absorption at 225 nm and 270 nm.

Optimization of RGO-PSS composite on GC electrode.

The current response of the BR sensor is influenced by the volume of RGO-PSS composite on GC surface and pH of the buffer. The current response increased with the increasing volume of composite and reached a summit at a volume of 7 µL of RGO-PSS (1mg/mL), and afterwards response current decreased upon increasing volume of composite which is shown in Fig. 3A. The pH of the buffer also plays a vital role in the performance of BR biosensor. To determine optimum pH, the pH of reaction buffer was varied from pH 7.0 to 9 at an

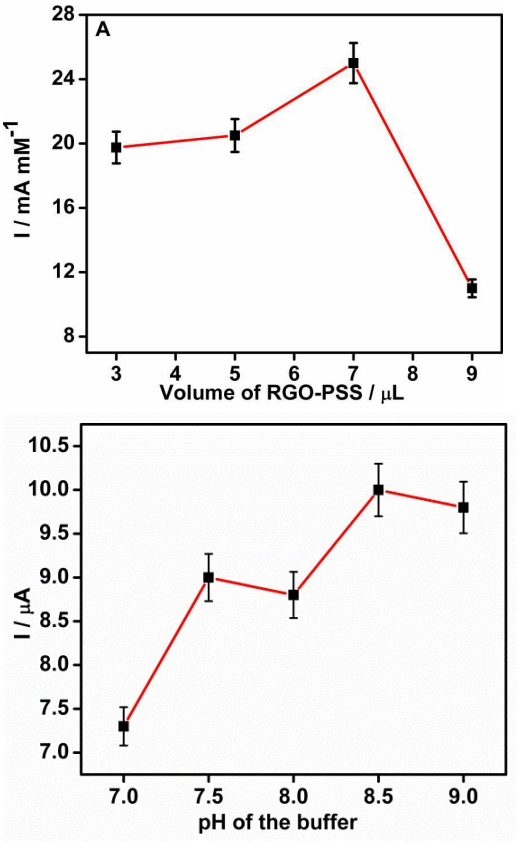

Fig.3. Optimization studies of the experimental conditions for the electro catalytic oxidation of BR. (A) The corresponding response of the BR biosensor through the optimization of RGO-PSS volume on the GC electrode. (B) The CV response of BR at different pH in Tris-HCl buffer.

interval of pH 0.5 using Tris-HCl buffer where the high current response has been observed at pH 8.5 as shown in Fig. 3B. So in our experiments, we used the optimized volume of RGO-PSS (7 µL) in all experiments while maintaining a pH of 8.5.

Electrocatalytic oxidation of Bilirubin

Initially, the surface area of the modified GC electrode was measured in 0.1M of KCl containing 1mM of K_3 [Fe $(CN)_6$] solution. A pair of well-defined oxidation and reduction peaks were obtained characteristic of the [Fe $(CN)_6]^{3-/4-}$ redox couple. The electrochemical surface area was calculated based on the Randles-Sevcik [26] equation.

$$Ip = 2.69 \times 105\ AD^{1/2}\ n^{3/2}\ \gamma^{1/2}\ C$$

A, electro active surface area (cm^2)

D, the diffusion coefficient of K_3 [Fe $(CN)_6$] in solution (6.70 × 10^{-6} cm^2 s^{-1})

n, the number of electrons participating in the redox reaction (for $[Fe(CN)_6]^{3-/4-}$, n = 1),

γ, the scan rate of the potential perturbation (V s^{-1})
C, the bulk concentration of the redox probe (mol cm^{-3}).

The calculated surface area of the electrodes showed the following trend:
Bare GCE (0.0627 cm^2) < RGO/GCE (0.0731 cm^2) < RGO-PSS/GCE (0.1271 cm^2).The trend suggests that RGO-PSS composite can enlarge the active surface area because of its three-dimensional structure.
The electro catalytic effect of RGO-PSS modified electrode towards the oxidation of bilirubin was investigated with the modified electrode (GC/RGO-PSS) as working electrode, NCE as reference and Pt foil as counter electrode. The background responses of the GC, GC/RGO and GC/RGO-PSS electrodes in Tris-HCl buffer alone showed no redox feature in the absence of bilirubin. In the presence of bilirubin (20 µM), a new anodic peak at 340 mV was observed due to oxidation of bilirubin (BR) to biliverdin (BV). The best electrochemical response has been registered in the CVs in the presence of GC-RGO-PSS modified electrode rather than bare GC electrode. The highest anodic peak current was obtained in the presence of RGO-PSS composite modified electrode due to its higher catalytic activity towards bilirubin oxidation (16 times that of bare GC and 2.5 times that of GC-RGO modified electrode) revealing that the GC-RGO-PSS composite film has large effective surface area and could provide a conducting path through the composite matrix for faster kinetics of electron transfer as shown in Fig. 4A. A weak anodic response for the oxidation of BR was also observed around 170 mV. However, it was not useful for analytical applications. Similarly the effect of substrate concentration on sensor response was investigated by varying the concentration of bilirubin in the range 2.48 µM–12.2 µM. The peak current increases with increasing bilirubin concentration due to oxidation of BR to BV and a good current response (in µA) was observed at 340 mV as shown in Fig. 4B. The weak anodic response observed at 170 mV was not quantitative. Hence subsequently amperometry studies were carried out 340 mV. The amperometry current response was investigated with increasing concentrations of bilirubin (5 - 90 µM) at the applied potential of 0.34 V vs SCE (1M KCl) as shown in Fig.5A. Inset shows the linear variation of bilirubin oxidation current with bilirubin concentration during each addition of bilirubin in a 5mL of Tris-HCl buffer solution. The steady state current of the RGO-PSS modified electrode could attain 90 % within 3 seconds after the addition of BR. I–t plot of RGO-PSS modified electrode shows significantly enhanced

sensitivity and linear range than bare GC electrode response for BR sensor (SI Fig. S2 B). The linear dynamic range was observed at normal bilirubin levels ranging between 5 and 45 µM in the case of bare GC electrode and 0-90 µM in the case of RGO-PSS electrode. The RGO-PSS modified electrode has potential stability for bilirubin oxidation even after 30days.

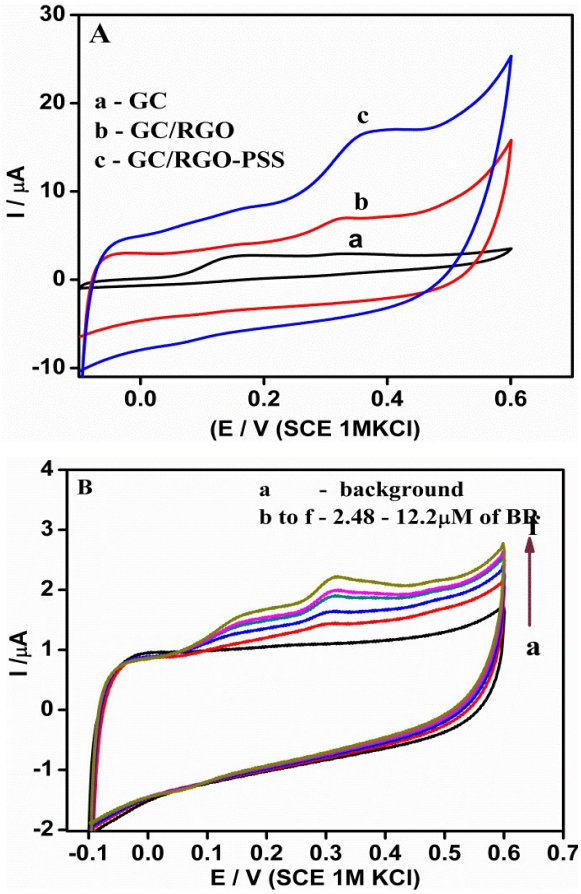

Fig.4. (A) CVs of (a) GC, (b) GC-RGO, (c) GC/RGO-PSS modified electrode in the Presence of bilirubin (20µM) at 50mV/s and (B) CVs of GC/RGO-PSS modified electrode in presence of BR (2.48-12.2 µM) in Tris-HCl pH - 8.5 at 50mV/s.

The detection limit of the sensor was 2 µM (calculated using the formula LOD = 3σ / slope) [27] with a sensitivity of 0.16 µA μM^{-1} cm^{-2} and a R^2 = 0.989 (ratio of signal to noise S/N=3). The detection limit of the BR sensor using bare GC was 7 µM with sensitivity of 0.004 µA µM-1 cm^{-2} and R^2 = 0.962.

Interference study of biosensor

In order to assess the possibility of interference of related bio-compounds, the current response was measured using amperometry in the presence of bilirubin (a-f – each addition corresponds to 2 µM) and other analytes such as ascorbic acid, (AA – 50 µM), hydrogen peroxide (H_2O_2 – 50 µM), glucose (Glu – 100 µM) and cholesterol (Cho - 100 µM) (Fig. 5B). The sensor response was not at all affected by the presence of other analytes in the normal physiological concentrations. The anionic surface of the modified electrode repels the ascorbic acid. The selectivity exhibited by the RGO-PSS modified GC indicates its potential for BR sensing compared to bare GC electrode which shows interferences with related bio-compounds as shown in supporting information (SI Fig S2 C).

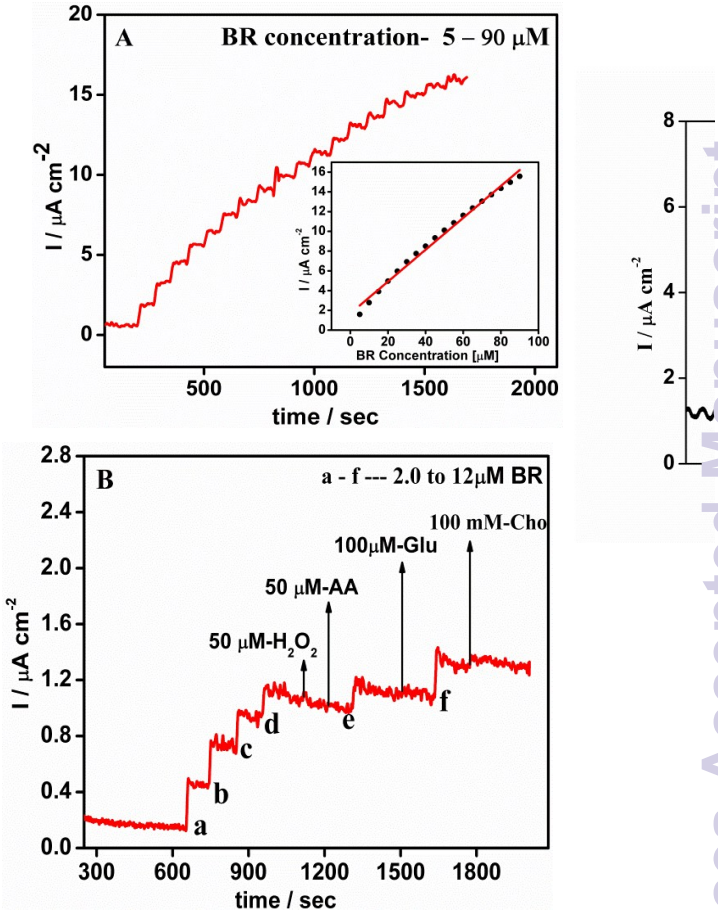

Fig.5 (A) Chronomperometry response of bilirubin (5-90 µM) at E_{app} = 340mV. Inset calibration plot of current vs BR concentration. (B) Interference effect with successive addition of H_2O_2, AA, Glucose and Cholesterol with bilirubin; a,b,c,d ,e and f correspond to the addition of bilirubin.

Measurements in the presence of Albumin

In human plasma, Bilirubin exits in two forms, conjugated and unconjugated BR. Conjugated bilirubin complexes with glucoronic acid and is water soluble. Unconjugated bilirubin tends to bind to albumin and therefore the amount of free unconjugated bilirubin depends on the concentration of albumin. The normal range of total bilirubin level in healthy adult person is 0.3 mg (5 µM) -1.9 mg/dl (32 µM) and the critical range of unconjugated BR for healthy newborn is greater than 15 mg/dl (200 µM), and goes up to 30 mg/dl (500 µM). The electrochemical behaviour of GC/RGO-PSS modified electrode in the presence of albumin was studied to measure BR in realistic conditions.

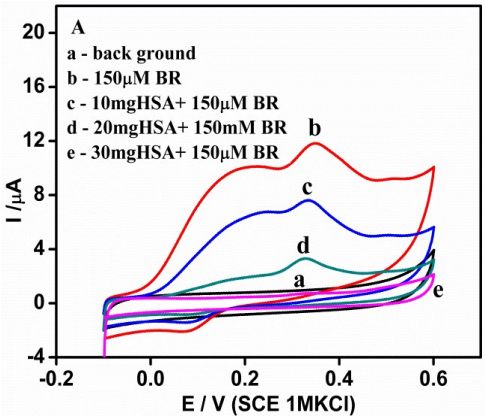

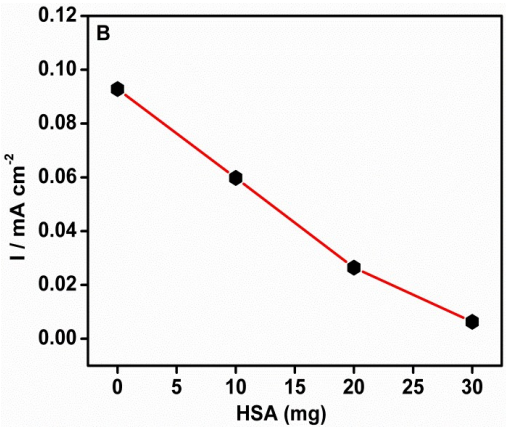

Fig.6 (A) Cyclic voltammograms of BR oxidation (150 μM) in the presence of different albumin concentration at 50 mV/s. [B] Calibration plot of current vs HSA ratio at fixed BR concentration (150 μM).

A fixed concentration of BR (150 μM) was mixed with human serum albumin in steps till the concentration equivalent to the normal value (30 mg/ml) was reached and CVs were recorded to see the influence of albumin on the electrochemical oxidation of BR. A reduction in the current signal was registered as shown in Fig. 6A. This behaviour can be explained by the decline of free BR in the presence of albumin. The oxidation current drops to a great extent in presence of albumin. It is most evident that the bilirubin is bound with albumin forming electro inactive complex. The influence of albumin concentration varying from 0, 10, 20 and 30 mg/ml on the oxidation current of BR (150 μM) is shown clearly in Fig. 6B. Beyond 150 μM, bilirubin remains free and can be detected using the RGO-PSS modified GC electrode. The complex formation between BR and HSA is confirmed by UV-Vis spectroscopic technique also and is presented in SI. (Fig. S3). Absorbance of BR and HSA were observed at 430 nm and 290 nm respectively. The mixture of BR and HSA shows red shift to 463 nm indicating the formation of complex. Fig. 7A shows the effect of BR (>150 μM) oxidation in presence of normal levels of human serum albumin. From Fig. 7A, it is clear that up to a BR concentration of 150 μM, which is the maximum concentration of BR, required to complex with 30mg/ml of HSA, the BR oxidation current is nearly absent.

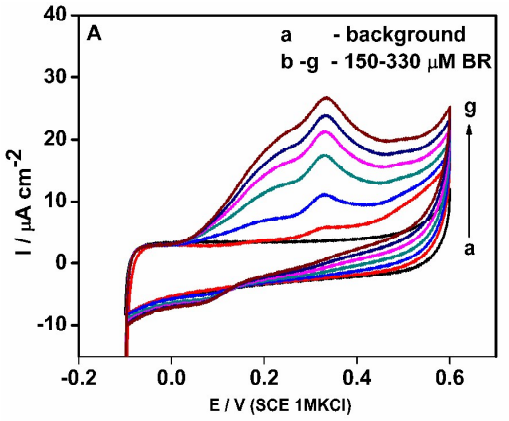

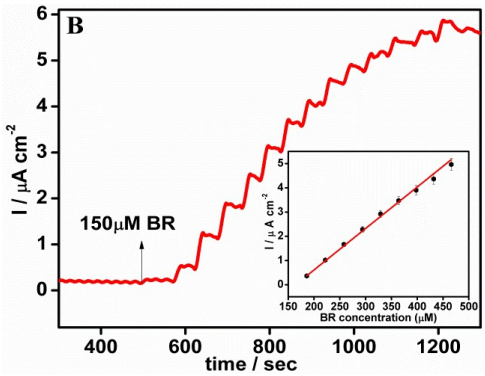

Fig.7 (A) Cyclic voltamograms of BR detection (150 - 330 μM) in the presence of albumin (30 mg of HSA) at 50mV/s. (B) Chronoamperometry was recorded with increasing BR concentrations (150 - 600 μM). Inset Calibration plot of current vs BR concentration.

Beyond this concentration, BR exists as free unconjugated BR and is responsible for several disorders as mentioned in the introduction section. The CVs presented in Fig.7A reveal that the free unconjugated BR (beyond the concentration of 150 μM) is electro active in presence of human serum albumin and its oxidation current increases gradually on the RGO-PSS modified GC electrode. Fig.7B represents the amperometric curve obtained for the free unbound BR for every 35 μM addition of BR. The BR oxidation current increases proportionally with BR concentration up to 600 μM and the inset of Fig. 7B shows the linear variation between the BR oxidation current and BR concentration. Since the bilirubin remains inactive upto 150 μM, the actual linear range of detection is 0-450 μM. In the presence of HSA, the sensor shows a sensitivity of 0.016 μA μM^{-1} cm^{-2} with a correlation coefficient of 0.990. The adsorption of proteins like serum albumin onto the electrode surface, decrease the sensor response, compared to the response of the RGO-PSS/GC electrode in the absence of albumin.

The measurement of free unbound BR is of great interest for clinicians for the diagnosis and treatment of certain diseases and is the parameter normally associated with the most serious clinical disorders [28]. In particular, the highest BR levels have been registered in neonatal jaundice. (Critical range: > 200 µM) and are linked to permanent brain damages. Therefore, experiments in this concentration range were performed with solutions containing relative physiological levels (30 mg/ml) of albumin and our experiments clearly show the usefulness of our technique to detect free unconjugated BR in case of neonatal jaundice and hyperbilirubinemia

A comparison of detection potential, linear range, detection limit, interference of related bio compounds of RGO-PSS/GC with other BR sensors reported in the literature are shown in Table1. The analytical performance of RGO-PSS composite modified electrode for BR sensor is comparable and even better than the reported values. Therefore RGO-PSS modified GC electrode is a better candidate for selective, non-enzymatic and stable bilirubin sensor with a wide linear range. The proposed BR sensor is useful to detect relative critical concentration range of jaundice level.

Real sample analysis

To investigate the potential application of the constructed non enzymatic bilirubin biosensor, it was used for bilirubin assay in a human blood serum sample. The determination of bilirubin content in a serum sample was carried out by amperometry as shown in Fig. 8.

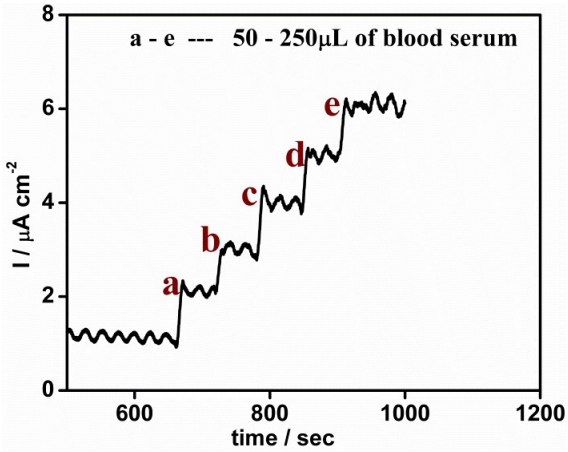

Fig.8. Chronoamperometry for BR detection in a serum sample. Each addition corresponds to 50µL of blood serum.

The current – time plot was obtained for the bilirubin sensor using GC/RGO-PSS modified electrode during the addition of 50 µL of human serum sample in 5mL of Tris-HCl buffer solution. Human serum sample was obtained by centrifuging the blood sample at 3000 rpm. The addition of serum was made five times. Equal increase in the current levels was observed for each addition of serum sample indicating the performance of GC/RGO-PSS modified electrode was satisfactory to the determination of bilirubin.

For further evaluation of the protocol, bilirubin is spiked into the blood serum and the % recovery of bilirubin was found to be > 97% (SI, Table 1)

Table.1 Comparison of the analytical parameters obtained at GCE/RGO-PSS with previously reported blirubin sensors

S/No	Electrode material	Detection potential (V vs SCE)	Linear range (µM)	Detection limit (µM)	Ref.
1	GCE/MWCNT-COOH/GNs/BOD	0.45	1.3 – 71.56	0.34	15
2	Poly TTCA/Mn (II)/PEI/AsOX	0.4	0.1 - 50	0.04	1
3	GCE/AuNs/MWCNT/Fc	0.45	1 - 100	0.12	29
4	GCE/MWCNT-COOH	0.3	-	9.4	5
5	GCE/Mn-Cu/Nf	0.4	1.2 - 420	0.025	30
6	GCE/RGO-PSS	0.34	Up to 315	2	Our work

Conclusion

The Non-enzymatic bilirubin sensor proposed in this study based on the RGO-PSS composite modified GC electrode. exhibited much better catalysis and higher sensitivity for the detection of free unconjugated bilirubin and displayed long-time stability (more than two months). The GC/RGO-PSS modified electrode could oxidise free unconjugated bilirubin at low overpotential. The detection of bilirubin was found to be free from interferences arising due to related compounds existing in biological environments. Linear calibration curves can be obtained in the relevant linear range of normal concentration of BR 0.3 mg/dL - 1.9 mg/dL and hyperbilirubinemia (Jaundice level in blood) ≥ 150 µM in the presence of human serum albumin (30 mg/mL). The wide linear range indicates that this modified electrode has a potential application to determine free unconjugated bilirubin level in blood serum which is a marker for bilirubin toxicity.

Acknowledgement

The authors acknowledge the funding received from the project “Molecules to materials to devices (M2D), CSC 0134 for carrying out this work

References

1. M. A. Rahman, K.-S. Lee, D.-S. Park, M.-S. Won and Y.-B. Shim, Biosens. Bioelectron., 2008, 23, 857–64.
2. S. Sarkar, A. Makhal, S. Baruah, M. A. Mahmood, J. Dutta and S. K. Pal, J phys.chem. C, 2012, 116, 9608–9615.
3. S.-K. Chou and M.-J. Syu, Biomaterials, 2009, 30, 1255–62.
4.G. Baydemir, M. Andaç, N. Bereli, R. Say and A. Denizli, Ind. Eng. Chem. Res., 2007, 46, 2843–2852.
5. I. Taurino, V. Van Hoof, G. De Micheli and S. Carrara, Thin Solid Films, 2013, 548, 546–550.
6. B. Batra, S. Lata, Sunny, J. S. Rana and C. S. Pundir, Biosens. Bioelectron., 2013, 44, 64–9.
7. X. Wang, J. R. Chowdhury and N. R. Chowdhury, Curr. Paediatr., 2006, 16, 70–74.
8. B. T. Doumas, B. W. Perry, E. A. Sasse and J. V Straumfjord, Clin. Chem., 1973, 19, 984–993.
9. X. Li and Z. Rosenzweig, Anal. Chim. Acta, 1997, 353, 263–273.
10. J. E. Chetn, J. Electroanal. Chem, 1985, 185, 61–71.
11. M. Santhosh, S. R. Chinnadayyala, A. Kakoti and P. Goswami, Biosens. Bioelectron., 2014, 59, 370–376.
12. J. Wang and M. Ozsoz, Electroanalysis, 1990, 2, 647–650.
13. A. Fortuney and G. G. Guilhault, Electroanalysis, 1996, 8, 3–6.
14. B. Shoham, Y. Migron, A. Riklin, I. Willner and B. Tartakovsky, Biosens. Bioelectron., 1995, 10, 341–352.
15. Q. Feng, Y. Du, C. Zhang, Z. Zheng, F. Hu, Z. Wang and C. Wang, Sensors Actuators B Chem., 2013, 185, 337–344.
16. M. A. Raj and S. A. John, J. Phys. Chem. C, 2013, 117, 4326–4335.
17. Y. Zhu, S. Murali, W. Cai, X. Li, J. W. Suk, J. R. Potts and R. S. Ruoff, Adv. Mater., 2010, 22, 3906–24.
18. M. K. Ram, P. Bertoncello, H. Ding, S. Paddeu and C. Nicolini, Biosens. Bioelectron., 2001, 16, 849–856.
19. R. Manjunatha, G. S. Suresh, J. S. Melo, S. F. D’Souza and T. V. Venkatesha, Sensors Actuators B Chem., 2010, 145, 643–650.
20. S.Prasannakumar, R. Manjunatha, C. Nethravathi, G. S. Suresh, M. Rajamathi and T. V Venkatesha, Port. Electrochim. Acta, 2012, 30, 371–383.
22. K. Wang, J. Ruan, H. Song, J. Zhang, Y. Wo, S. Guo and D. Cui, Nanoscale Res. Lett., 2010, 6, 8.
23. J. Luo, S. Jiang, R. Liu, Y. Zhang and X. Liu, Electrochim. Acta, 2013, 96, 103–109.
24.L. Li, R. Ma, N. Iyi, Y. Ebina, K. Takada and T. Sasaki, Chem. Commun. (Camb). 2006, 2, 3125–7.
25. J. Tian, H. Li, Z. Xing, L. Wang, Y. Luo, A. M. Asiri, A. O. Al-Youbi and X. Sun, Catal. Sci. Technol., 2012, 2, 2227.
26. Y. Zhang, X. Bai, X. Wang, K. Shiu, Y. Zhu and H. Jiang, Anal. Chem., 2014, 86, 9459–9465.
27. I. Union, O. F. Pure and A. Chemistry, Pure Appl. Chem., 1997, 69, 297–328.
28.Y. Andreu, M. Ostra, C. Ubide, J. Galba, S. De Marcos and J. R. Castillo, Talanta, 2002, 57, 343–353.
29. C. Wang, G. Wang and B. Fang, Microchim. Acta, 2008, 164, 113–118.
30. H.-B. Noh, M.-S. Won and Y.-B. Shim, Biosens. Bioelectron., 2014, 61, 554–61.